crystals

MDPI

Article

Synthesis, Characterization and Single Crystal X-ray Diffraction Analysis of Fused Triazolo/Thiadiazole Clubbed with Indole Scaffold

Mezna Saleh Altowyan [1], Matti Haukka [2], Saied M. Soliman [3], Assem Barakat [4,*], Saleh O. Alaswad [5], Ahmed T. A. Boraei [6,*], Emad M. Gad [6] and Mohamed F. Youssef [6,*]

1 Department of Chemistry, College of Science, Princess Nourah bint Abdulrahman University, P.O. Box 84428, Riyadh 11671, Saudi Arabia
2 Department of Chemistry, University of Jyväskylä, P.O. Box 35, FI-40014 Jyväskylä, Finland
3 Chemistry Department, Faculty of Science, Alexandria University, P.O. Box 426, Alexandria 21321, Egypt
4 Department of Chemistry, College of Science, King Saud University, P.O. Box 2455, Riyadh 11451, Saudi Arabia
5 Nuclear Science Research Institute (NSRI), King Abdulaziz City for Science and Technology (KACST), P.O. Box 6086, Riyadh 11442, Saudi Arabia
6 Chemistry Department, Faculty of Science, Suez Canal University, Ismailia 41522, Egypt
* Correspondence: ambarakat@ksu.edu.sa (A.B.); ahmed_tawfeek83@yahoo.com or ahmed_boraei@science.suez.edu.eg (A.T.A.B.); mohamed_gomaa@science.suez.edu.eg (M.F.Y.); Tel.: +966-11467-5901 (A.B.); Fax: +966-11467-5992 (A.B.)

Abstract: The present synthetic strategy involves the synthesis of indolyl-triazolo-thiadiazole heterocyclic ring systems **8**–**13** from the condensation of 4-amino-5-(1*H*-indol-2-yl)-3*H*-1,2,4-triazole-3-thione **1** with the aromatic carboxylic acid derivatives **2**–**7** in presence of $POCl_3$ for 1 h. All compounds were obtained in very good yields and have been well-characterized using spectroscopic techniques. Exclusively, good quality crystals from the target organic hybrid 8-(1*H*-indol-2-yl)-5-(*p*-tolyl)-[1,2,4]triazolo [3,4-b][1,3,4]thiadiazole **9** were obtained and found suitable for X-ray single crystal diffraction measurement, which is used to confirm and analyze the molecular and supramolecular structure aspects of **9**. The solid-state structure of the synthesized molecule **9** agrees very well with other characterizations. The packing of **9** is dominated by the N . . . H, S . . . H, C . . . C and S . . . C non-covalent interactions, which agree with the Hirshfeld surface analysis. The percentages of these contacts are calculated to be 20.3%, 5.4%, 9.4% and 4.3%, respectively.

Keywords: fused heterocycle; triazole; thiadiazole; computational study

Citation: Altowyan, M.S.; Haukka, M.; Soliman, S.M.; Barakat, A.; Alaswad, S.O.; Boraei, A.T.A.; Gad, E.M.; Youssef, M.F. Synthesis, Characterization and Single Crystal X-ray Diffraction Analysis of Fused Triazolo/Thiadiazole Clubbed with Indole Scaffold. *Crystals* **2023**, *13*, 423. https://doi.org/10.3390/cryst13030423

Academic Editor: Volodymyr Bon

Received: 4 February 2023
Revised: 19 February 2023
Accepted: 23 February 2023
Published: 1 March 2023

1. Introduction

Indole chemistry is a wonderful area of research and has gained a lot of attention from researchers for centuries. This fused heterocycle pharmacophore ring exists in many biological hits, which makes this unit a privileged molecule [1]. The indole core structure is found in alkaloid polycyclic compounds and has shown broad-spectrum actions in many pharmacological applications. Among their biological activities, these compounds have been applied as targeting enzyme inhibitors in cancer research, specifically PARP-1 and EGFR inhibitors [2–4], α-glucosidase inhibitor [5] and anti-HIV (anti-human immunodeficiency virus) [6], and have also exhibited other activities, including anti-microbial [7], anti-inflammation [8], anti-vascular [9], ischemia/reperfusion injury [10], and anti-malarial potential [11].

On the other hand, the 4-amino-1,2,4-triazole-3-thione motif is an interesting scaffold that can be utilized for the synthesis of heterocyclic compounds via annulation or Schiff base formation because it has good functionality. This pharmacophore showed interesting biological patterns, including anti-tumor [12], anti-malarial [13], anti-microbial [14], anti-convulsant [15], and anti-proliferative behaviors [16]. Additionally, it has been used as an

enzyme inhibitor, such as for protein tyrosine phosphatase 1B [17], AChE enzyme [18], urease enzymes [19] and dizinc metallo-β-lactamase [20]. L. Gavara et al. have designed and synthesized a new Schiff base derived from the 4-amino-1,2,4-triazole-3-thione core structure, which showed high efficacy and more selectivity against metallo-β-lactamases (MBLs) [21]. Recently, Boraei et al. [22] utilized this synthon combined with indole moiety for annulation, and yielded a new triazolo/thiadiazole heterocycle with a confirmed molecular structure, which makes this scaffold interesting and will lead to further research. Triazole and fused rings have shown great biological importance in the medical chemistry and drug discovery research fields [23–27].

The chemical insights yielded by the newly synthesized molecules have attracted the attention of many researchers. One of the most powerful tools that can provide insights into the intermolecular interactions in molecular crystals is Hirshfeld surface analysis. The shape- and size-based Hirshfeld surface analysis approach allows the quantitative and qualitative exploration and visualization of the intermolecular contacts in crystalline molecules. In this context, based on the findings mentioned above and in continuation of our research program focused on heterocyclic chemistry [28–30], we have synthesized new fused triazolo/thiadiazole heterocycles combined with an indole scaffold. The molecular structures of the desired molecules are fully characterized based on spectrophotometric tools, in addition to single-crystal X-ray diffraction (SCXRD) analysis. Hirshfeld surface analysis has also been performed.

2. Materials and Methods

2.1. General

Melting points were measured via a melting point apparatus (SMP10) with open capillaries and are inclded uncorrected. Nuclear magnetic resonance (^{1}H-NMR and ^{13}C-NMR) spectra were determined using DMSO-d_6 on Bruker AC 300 and 400 MHz spectrometers, respectively, in the presence of tetramethylsilane as an internal standard. Chemical shifts are described in δ (ppm) and coupling constants are given in Hz. Elemental analysis was performed on a Flash EA-1112 instrument. A Finnigan MAT 95XP was used to record the mass spectra of HREI experiments. A Jeol JMS HX110 mass spectrometer was used to capture the FAB-MS data.

2.2. General Procedures

A mixture of 3.0 mmol of appropriate aromatic carboxylic acid derivative **2**–**7** (3.0 mmol) was refluxed in 10 mL phosphorus oxychloride for 1 h, then left to cool to room temperature, before being poured over ice water. The formed precipitates were collected by filtration, dried and recrystallized from DMF to produce the pure compounds **8**–**13**. Only 8-(1*H*-indol-2-yl)-5-(*p*-tolyl)-[1,2,4]triazolo [3,4-b][1,3,4]thiadiazole 9 was obtained in a sufficient crystal form for SCXRD measurement.

8-(1*H*-Indol-2-yl)-5-phenyl-[1,2,4]triazolo [3,4-*b*][1,3,4]thiadiazole 8

Yield: 87%, m.p. > 300 °C; ^{1}H NMR (DMSO-d_6, 300 MHz) δ 7.09 (dd, *J* = 7.8, *J* = 7.2 Hz, 1H), 7.22 (dd, *J* = 7.2, *J* = 7.8 Hz, 1H), 7.47–7.72 (m, 6H), 8.13 (d, *J* = 6.6 Hz, 2H), 12.13 (br.s, 1H); ^{13}C NMR (DMSO-d_6, 75 MHz) δ 102.67, 111.97, 119.88, 121.00, 122.27, 123.27, 127.30, 127.58, 128.95, 129.63, 132.95, 137.15, 141.13, 153.45, 167.01; HRMS (EI) calcd for $C_{17}H_{11}N_5S$ (M+): 317.0715. Found: 317.0726.

8-(1*H*-Indol-2-yl)-5-(*p*-tolyl)-[1,2,4]triazolo [3,4-*b*][1,3,4]thiadiazole 9

Yield: 83%, m.p. > 300 °C; ^{1}H NMR (DMSO-d_6, 400 MHz) δ 2.42 (s, 3H), 7.08 (dd, *J* = 8.0, *J* = 7.5 Hz, 1H), 7.22 (dd, *J* = 7.5, *J* = 8.4 Hz, 1H), 7.45–7.51 (m, 4H), 7.71 (d, *J* = 8.0 Hz, 1H), 7.99 (d, *J* = 8.0 Hz, 2H), 12.08 (br.s, 1H); ^{13}C NMR (DMSO-d_6, 100 MHz) δ 21.19, 102.69, 112.04, 119.95, 121.09, 122.94, 123.33, 126.31, 127.29, 127.66, 130.24, 137.21, 143.52, 167.13; HRMS (FAB +ve) calcd for $C_{18}H_{14}N_5S$ (M + 1): 332.0970. Found: 332.0955.

3-(1*H*-Indol-2-yl)-6-(4-methoxyphenyl)-[1,2,4]triazolo [3,4-*b*][1,3,4]thiadiazole 10

Yield: 82%, m.p. > 300 °C; ^{1}H NMR (DMSO-d_6, 400 MHz) δ 3.91 (s, 3H), 7.11 (t, *J* = 7.5 Hz, 1H), 7.18–7.31 (m, 3H), 7.40–7.58 (m, 2H), 7.73 (d, *J* = 7.9 Hz, 1H), 8.10 (d,

J = 8.8 Hz, 2H), 12.14 (s, 1H); ^{13}C NMR (DMSO-d_6, 100 MHz) δ 56.19, 103.15, 112.51, 115.57, 120.45, 121.56, 123.40, 123.53, 128.10, 129.70, 137.62, 141.51, 162.90, 163.40; elemental analysis calculated for [$C_{18}H_{13}N_5OS$]: C, 62.23; H, 3.77; N, 20.16; S, 9.23. Found: C, 62.34; H, 3.86; N, 20.08; S, 9.35.

8-(1*H*-Indol-2-yl)-5-(4-chlorophenyl)-[1,2,4]triazolo [3,4-*b*][1,3,4]thiadiazole 11

Yield: 92%, m.p. >300 °C; ^{1}H NMR (DMSO-d_6, 300 MHz) δ 7.09 (dd, *J* = 8.1, *J* = 7.2 Hz, 1H), 7.22 (dd, *J* = 7.2, *J* = 8.4 Hz, 1H), 7.46 (s, 1H), 7.49 (d, *J* = 8.4 Hz, 1H), 7.69–7.76 (m, 4H), 8.16 (d, *J* = 8.4 Hz, 2H), 12.13 (br.s, 1H); ^{13}C NMR (DMSO-d_6, 75 MHz) δ 102.74, 111.96, 119.96, 121.06, 122.81, 123.36, 127.61, 127.88, 129.12, 129.77, 137.20, 137.66, 141.18, 153.60, 165.97; HRMS (FAB +ve) calcd for $C_{17}H_{11}N_5SCl$ (M+1): 352.0424. Found: 352.0441.

6-(2-Bromophenyl)-3-(1*H*-indol-2-yl)-[1,2,4]triazolo [3,4-*b*][1,3,4]thiadiazole 12

Yield: 73%, m.p. 296–297 °C; ^{1}H NMR (400 MHz, DMSO) δ 7.11 (d, *J* = 7.2 Hz, 1H), 7.24 (d, *J* = 8.1 Hz, 1H), 7.43 (d, *J* = 1.4 Hz, 1H), 7.52 (d, *J* = 8.3 Hz, 1H), 7.84–7.62 (m, 4H), 8.25 (dd, *J* = 7.7, 1.7 Hz, 1H), 12.18 (s, 1H); ^{13}C NMR (DMSO-d_6, 100 MHz) δ 103.30, 112.53, 120.47, 121.61, 121.88, 123.20, 123.93, 128.08, 129.09, 129.88, 132.87, 134.27, 134.71, 137.70, 141.60, 150.53, 165.88; elemental analysis calculated for [$C_{17}H_{10}BrN_5S$]: C, 51.53; H, 2.54; Br, 20.16; N, 17.67; S, 8.09. Found: C, 51.70; H, 2.55; Br, 20.18; N, 17.61; S, 8.13.

3-(1*H*-indol-2-yl)-6-(pyridin-3-yl)-[1,2,4]triazolo [3,4-*b*][1,3,4]thiadiazole 13

Yield: 77%, m.p. >300 °C; ^{1}H NMR (DMSO-d_6, 400 MHz) δ 7.19 (m, 2H), 7.52 (s, 2H), 7.73 (d. *J* = 7.5 Hz, 2H), 8.55 (s, 1H), 8.90 (s, 1H), 9.35 (s, 1H), 12.16 (s, 1H); ^{13}C NMR (DMSO-d_6, 100 MHz) δ 103.50, 112.56, 120.48, 121.58, 123.24, 123.89, 124.95, 128.17, 135.59, 137.78, 148.31, 153.76, 162.82, 165.17; elemental analysis calculated for [$C_{16}H_{10}N_6S$]: C, 60.36; H, 3.17; N, 26.40; S, 10.07. Found: C, 60.41; H, 3.13; N, 26.32; S, 10.11.

2.3. X-ray Structure Determinations

The technical procedure for the chemical structural elucidation of compound **9** via X-ray single-crystal diffraction analysis is given in the Supplementary Materials (The protocol and refinement crystal data Tables S1–S6). Crystal data were refined using the software from [31–34]. Table 1 lists the data regarding the synthesized crystals of compound **9**.

Table 1. Crystal data for **9**.

	9
CCDC	2239222
empirical formula	$C_{18}H_{13}N_5S$
fw	331.39
temp. (K)	120(2) K
λ(Å)	0.71073 Å
cryst syst	Monoclinic
space group	$P2_1/n$
a (Å)	*a* = 7.8707(2) Å
b (Å)	*b* = 15.9681(4) Å
c (Å)	*c* = 11.9798(4) Å
β (deg)	100.283(3)°
V (Å^3)	1481.44(7) Å^3
Z	4
ρ_{calc} (Mg/m^3)	1.486 Mg/m^3
μ(Mo Kα) (mm^{-1})	0.228 mm^{-1}
No. reflns.	7305
Unique reflns.	3997
Completeness to θ = 25.242°	100%
GOOF (F^2)	1.031
R_{int}	0.0213
R_1 [a] ($I \geq 2\sigma$)	0.0454
wR_2 [b] ($I \geq 2\sigma$)	0.1095

[a] $R_1 = \Sigma||F_o| - |F_c||/\Sigma|F_o|$. [b] $wR_2 = \{\Sigma[w(F_o^2 - F_c^2)^2]/\Sigma[w(F_o^2)^2]\}^{1/2}$.

2.4. Hirshfeld Surface Analysis

The Crystal Explorer 17.5 program was used to perform the topology analysis of studied compound **9** [35].

3. Results and Discussion

3.1. Chemistry and Characterizations

4-Amino-5-(1*H*-indol-2-yl)-3*H*-1,2,4-triazole-3-thione **1** was mixed separately with benzoic acid, *p*-toluic acid, anisic acid, *p*-chlorobenzoic acid, o-bromobenzoic acid and nicotinic acid **2**–**7** in $POCl_3$ for 1 h; this afforded the indolyl-triazolo-thiadiazoles **8**–**13**, respectively, in excellent yields (Scheme 1). ^{1}H- and ^{13}C-NMR exhibited the characteristic signals of aromatic protons, between 7.08 ppm and 8.28 ppm, whereas the aromatic carbons were found at 102.0–167.0 ppm. In addition, the NMR study of compound **9** showed the proton for the methyl group at 2.42 ppm, and the carbon of the methyl group at 21.19 ppm. Moreover, the NMR of compound **10** revealed methoxy protons at 3.91 ppm and methoxy carbon at 56.19 ppm. Crystals suitable for the X-ray single-crystal analysis of compound **9** were obtained via recrystallization from DMF.

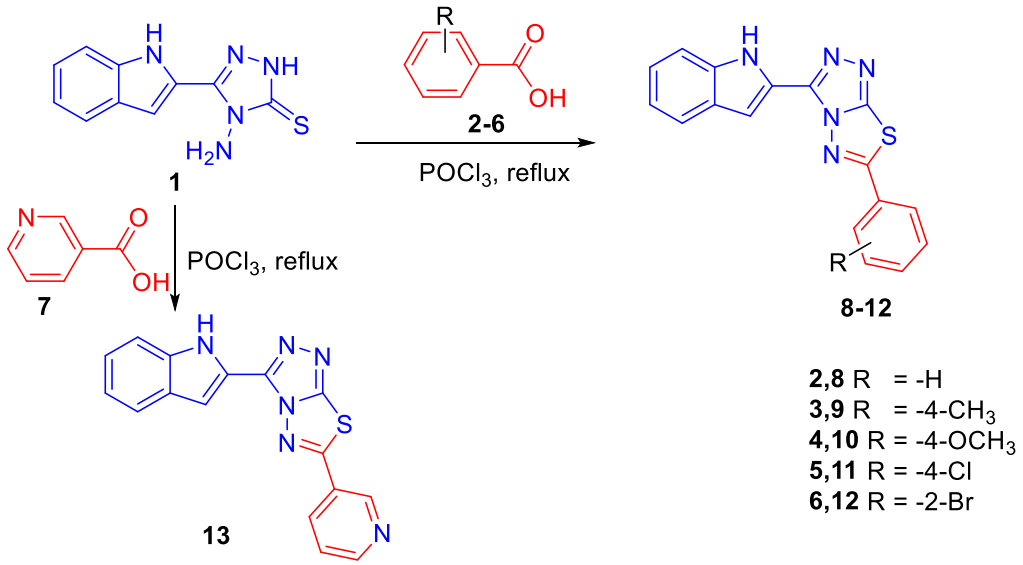

Scheme 1. Synthesis of the target fused heterocycles.

3.2. Crystal Structure Description

Figure 1 shows the molecular structure of compound **9**, obtained by single-crystal X-ray diffraction analysis. Table 1 lists some of the selected bon angles and bond distances of the desired compound. The monoclinic system was observed in the crystallized compound and centrosymmetric $P2_1/n$ space group, with lattice parameters $a = 7.8707(2)$ Å, $b = 15.9681(4)$ Å, $c = 11.9798(4)$ and $\beta = 100.283(3)^\circ$. The asymmetric unit contained one molecule, while the unit cell comprised four molecules. The crystal density was 1.486 Mg/m^3 and the unit cell volume was 1481.44(7) Å^3. The molecule comprised a number of aromatic ring systems, which were perfectly planar but showed some twists. The phenyl group of the aryl moiety was twisted from the mean plane of the fused aromatic ring system (**A**) by only 2.85°. The two fused ring systems **A** and **C** were nearly coplanar with one another. The twist angle between the mean plane of the two fused ring systems was only 0.60°. Selected bond lengths and angles are depicted in Table 2.

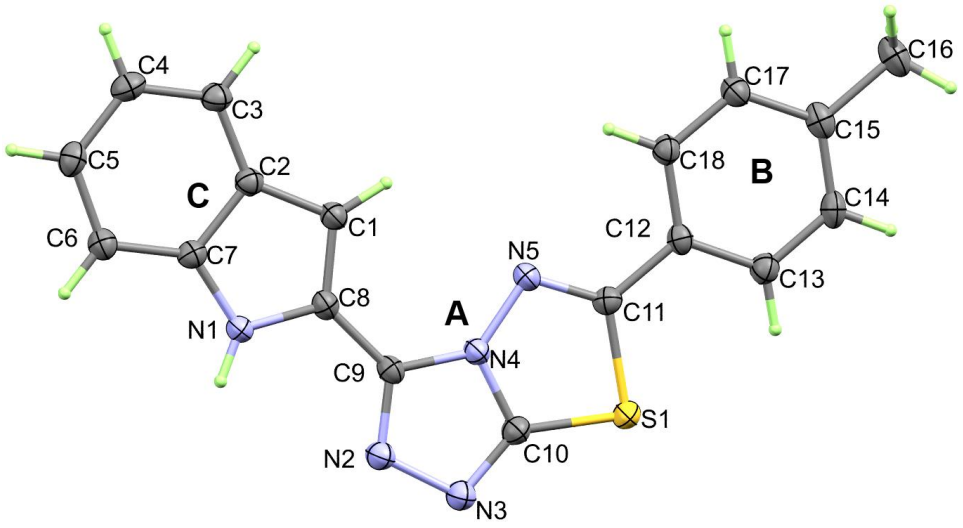

Figure 1. ORETP of crystalized compound **9**.

Table 2. Bond lengths (Å) and angles (°) of **9**.

Bond	Length/Å	Bond	Length/Å
S(1)-C(10)	1.7275(18)	N(3)-C(10)	1.306(2)
S(1)-C(11)	1.7734(17)	N(4)-C(10)	1.360(2)
N(1)-C(7)	1.376(2)	N(4)-C(9)	1.370(2)
N(1)-C(8)	1.381(2)	N(4)-N(5)	1.3747(19)
N(2)-C(9)	1.324(2)	N(5)-C(11)	1.304(2)
N(2)-N(3)	1.402(2)		
Bonds	**Angle/°**	**Bonds**	**Angle/°**
C(10)-S(1)-C(11)	87.61(8)	N(1)-C(7)-C(6)	130.16(16)
C(7)-N(1)-C(8)	108.31(14)	N(1)-C(7)-C(2)	107.94(15)
C(9)-N(2)-N(3)	109.54(14)	N(1)-C(8)-C(9)	120.90(15)
C(10)-N(3)-N(2)	104.79(14)	N(2)-C(9)-N(4)	107.75(14)
C(10)-N(4)-C(9)	105.87(14)	N(2)-C(9)-C(8)	127.46(16)
C(10)-N(4)-N(5)	118.88(14)	N(4)-C(9)-C(8)	124.79(15)
C(9)-N(4)-N(5)	135.17(14)	N(3)-C(10)-N(4)	112.04(15)
C(11)-N(5)-N(4)	107.48(14)	N(3)-C(10)-S(1)	138.55(14)
N(5)-C(11)-S(1)	116.67(13)	N(4)-C(10)-S(1)	109.37(12)
C(1)-C(8)-N(1)	109.98(15)	N(5)-C(11)-C(12)	123.27(15)

The molecular units of this compound are controlled by a range of weak non-covalent interactions, including the N ... H, S ... H and C ... C interactions. The molecules are connected to each other by N1-H1 ... N2, N1-H1 ... N3 and C14-H14 ... S1 interactions (Table 3). The different N ... H and S ... H contacts are shown in Figure 2A, while the resulting packing scheme is presented in Figure 2B. Additionally, the packing of **9** is controlled by different levels of C ... C interactions, which are kinds of π–π stacking interactions (Figure 2C). The shortest C ... C interactions are depicted in Table 4.

Table 3. Hydrogen bonds for **9** (Å and °).

D-H ... A	d(D-H)	d(H ... A)	d(D ... A)	<(DHA)
N1-H1 ... N2#1	0.85(2)	2.12(2)	2.959(2)	169(2)
N1-H1 ... N3#1	0.85(2)	2.60(2)	3.292(2)	139(2)
C14-H14 ... S1#2	0.95	2.905	2.905	179.35

Symm. codes: #1 −x + 1, −y + 1, −z and #2 −1/2 + x, 1.5−y, −1/2 + z.

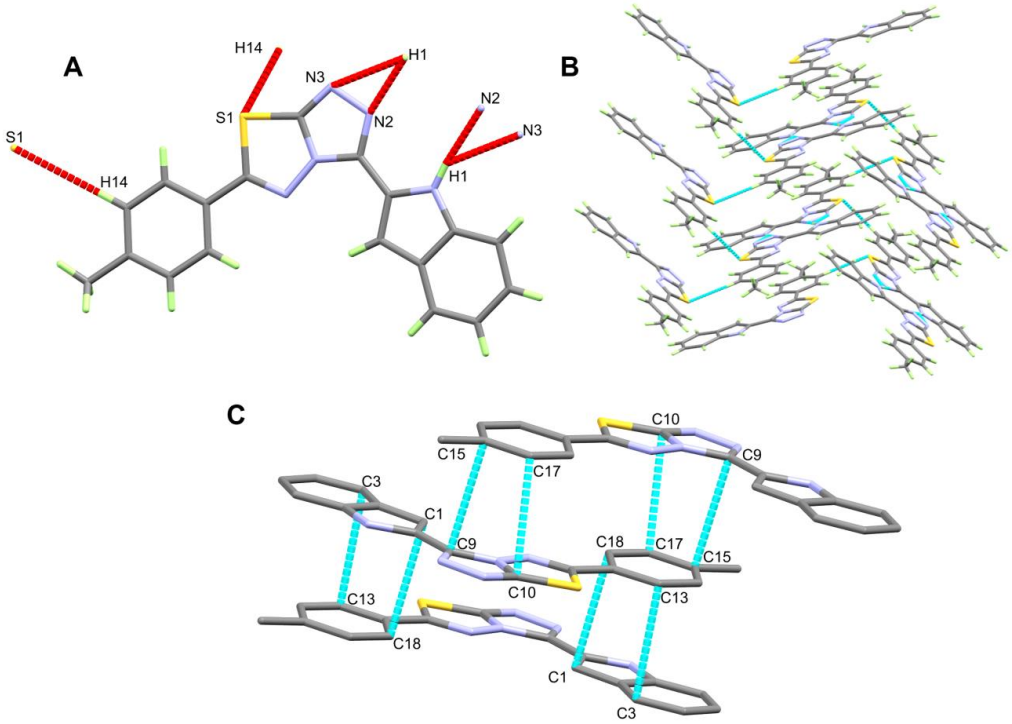

Figure 2. The N . . . H/S . . . H contacts (**A**), molecular packing view via N . . . H/S . . . H contacts (**B**) and π–π stacking interactions (**C**) for **9**.

Table 4. The shortest C . . . C for π–π stacking interactions.

Contact	Distance	Symmetry Code
C1 . . . C18	3.371	1 − x,1 − y,1 − z
C3 . . . C13	3.342	1 − x,1 − y,1 − z
C9 . . . C15	3.288	2 − x,1 − y,1 − z
C10 . . . C17	3.349	2 − x,1 − y,1 − z

3.3. Hirshfeld Surface Analysis

The stability of crystalline materials is controlled by different intermolecular interactions that occur among the adjacent molecules [36,37]. The types, strengths and weights of the intermolecular interactions in the crystal structure could be simply analyzed using Hirshfeld calculations. There are three important maps, which are the d_{norm}, shape index and curvedness maps. A view of these surfaces is shown in Figure 3. In the d_{norm} map, the presence of red regions indicates short contacts, which are considered of great importance to crystal stability.

The decomposition of the fingerprint plot gives the weight of each contact in the crystal structure, and also sheds light on the strength of each contact. The percentages of all contacts contributing to molecular packing are presented in Figure 4. The most important short contacts are the N . . . H, S . . . H, C . . . C and S . . . C interactions. Their percentages are calculated to be 20.3%, 5.4%, 9.4% and 4.3%, respectively. Decomposed fingerprint plots of these short contacts are shown in Figure 5. The majority of these interactions appeared in the fingerprint plots as sharp spikes, which confirms that that these interactions are important. A list of the short N . . . H, S . . . H, C . . . C and S . . . C contacts and their corresponding interaction distances is presented in Table 5. Other contacts contributed to a large extent in the molecular packing, including H . . . H and H . . . C interactions. The percentages of these interactions are 38.3% and 18.3%, respectively.

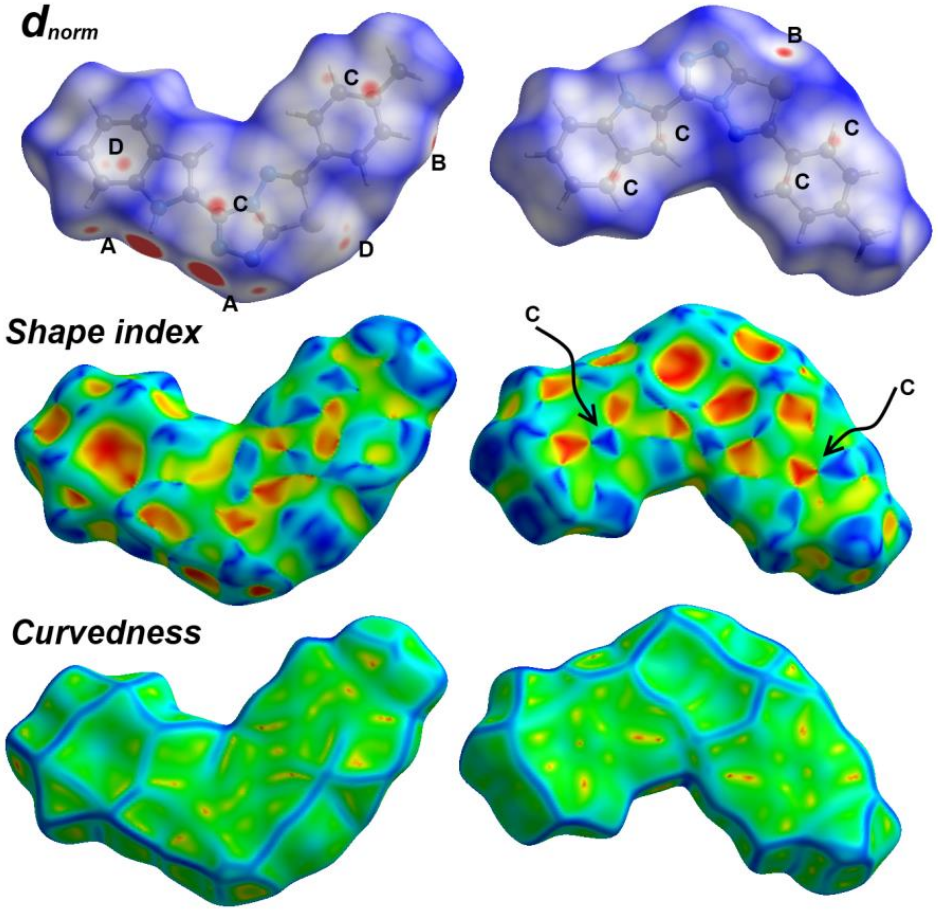

Figure 3. Hirshfeld surfaces of **9** showing the most important interactions: N . . . H (**A**), S . . . H (**B**), C . . . C (**C**) and C . . . S (**D**).

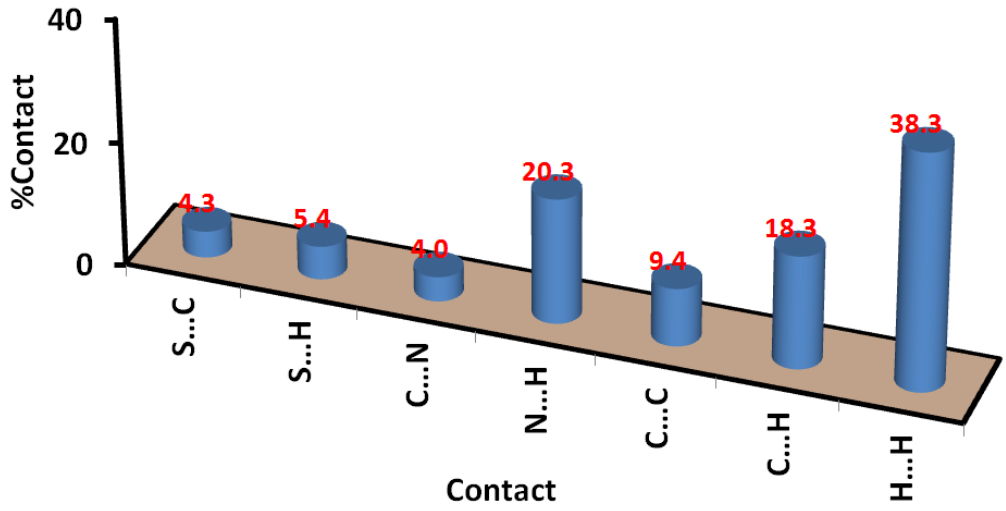

Figure 4. Intermolecular contacts and their percentages in **9**.

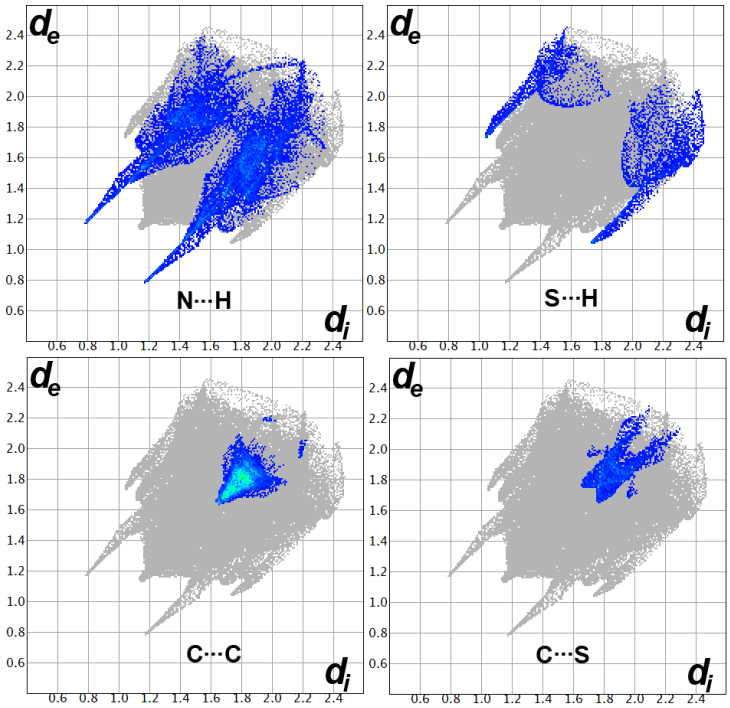

Figure 5. Decomposed fingerprint plots for the short contacts in **6**.

Table 5. Short contacts and the corresponding interaction distances.

Contact	Distance	Contact	Distance
N2 . . . H1	1.963	C9 . . . C15	3.288
N3 . . . H1	2.483	C10 . . . C17	3.349
N3 . . . H6	2.512	C6 . . . S1	3.469
S1 . . . H14	2.772	C7 . . . S1	3.42

Another important feature of molecular packing is the π–π stacking interactions. The presence of these types of intermolecular contact is indicated by the presence of short C9 . . . C15 (3.288 Å) and C10 . . . C17 (3.349 Å) interactions. Additionally, the presence of π–π stacking interactions is clearly implied by the presence of red/blue triangles and a flat green area in the shape index and curvedness maps, respectively (Figure 3).

4. Conclusions

New heterocyclic systems including indole, triazole amd thiadiazole rings **8**–**13** were synthesized from the reaction of 4-amino-5-(1*H*-indol-2-yl)-3*H*-1,2,4-triazole-3-thione and benzoic acid derivatives in $POCl_3$. The success of our strategy to design target compounds is proven by our obtaining of the hybrid heterocycle **9** in a good crystalline form. Its structure was revealed by measuring its X-ray single-crystal structure. The resulting X-ray structure was used to analyze the molecular packing of the newly synthesized compound **9**. Additionally, the type, strength and weight of the intermolecular interactions in the crystal structure were analyzed using Hirshfeld calculations. It was found that the N . . . H (20.3%), S . . . H (5.4%), C . . . C (9.4%) and S . . . C (4.3%) non-covalent interactions were the most important.

Supplementary Materials: The following supporting information can be downloaded at: https://www.mdpi.com/article/10.3390/cryst13030423/s1, X-ray determination protocol for compound **9** [31,33,34]. Table S1: Atomic coordinates ($\times 10^4$) and equivalent isotropic displacement parameters (Å2 $\times$ 10^3) for **9**. U(eq) is defined as one third of the trace of the orthogonalized Uij tensor; Table S2: Selected bond lengths [Å] and angles [°] for **9**; Table S3: Bond lengths [Å] and angles [°] for **9**; Table S4: Anisotropic

displacement parameters (Å2 × 10^3) for **9**. The anisotropic displacement factor exponent takes the form: −2p2[h2 a*2U11 + ... + 2 h k a* b* U12; Table S5: Hydrogen coordinates (×10^4) and isotropic displacement parameters (Å2 × 10^3) for **9**; Table S6: Torsion angles [°] for **9**.

Author Contributions: Conceptualization, A.B., A.T.A.B. and M.F.Y.; methodology, M.S.A., M.F.Y. and E.M.G.; software, M.H. and S.M.S.; formal analysis, M.S.A., A.T.A.B., M.F.Y., E.M.G. and S.O.A.; X-ray crystal structure: M.H.; investigation, M.S.A. and S.M.S.; resources, A.T.A.B., A.B. and M.S.A.; writing—original draft preparation, A.T.A.B., M.F.Y., E.M.G., S.M.S. and A.B.; data curation, S.O.A.; writing—review and editing: All authors have prepare. All authors have read and agreed to the published version of the manuscript.

Funding: Princess Nourah bint Abdulrahman University Researchers Supporting Project number (PNURSP2023R86), Princess Nourah bint Abdulrahman University, Riyadh, Saudi Arabia.

Data Availability Statement: Not applicable.

Acknowledgments: Princess Nourah bint Abdulrahman University Researchers Supporting Project number (PNURSP2023R86), Princess Nourah bint Abdulrahman University, Riyadh, Saudi Arabia.

Conflicts of Interest: The authors declare no conflict of interest.

References

1. Elshaier, Y.A.; Nemr, M.T.; Al Refaey, M.; Fadaly, W.A.; Barakat, A. Chemistry of 2-vinylindoles: Synthesis and applications. *New J. Chem.* **2022**, *46*, 13383–13400. [CrossRef]
2. Boraei, A.T.; Ghabbour, H.A.; Gomaa, M.S.; El Ashry, E.S.H.; Barakat, A. Synthesis and anti-proliferative assessment of triazolo-thiadiazepine and triazolo-thiadiazine scaffolds. *Molecules* **2019**, *24*, 4471. [CrossRef] [PubMed]
3. Boraei, A.T.A.; Gomaa, M.S.; El Sayed, E.S.H.; Duerkop, A. Design, selective alkylation and X-ray crystal structure determination of dihydro-indolyl-1,2,4-triazole-3-thione and its 3-benzylsulfanyl analogue as potent anticancer agents. *Eur. J. Med. Chem.* **2017**, *125*, 360–371. [CrossRef] [PubMed]
4. Boraei, A.T.; Ashour, H.K.; El Sayed, H.; Abdelmoaty, N.; El-Falouji, A.I.; Gomaa, M.S. Design and synthesis of new phthalazine-based derivatives as potential EGFR inhibitors for the treatment of hepatocellular carcinoma. *Bioorg. Chem.* **2019**, *85*, 293–307. [CrossRef]
5. Islam, M.S.; Barakat, A.; Al-Majid, A.M.; Ali, M.; Yousuf, S.; Choudhary, M.I.; Khalil, R.; Ul-Haq, Z. Catalytic asymmetric synthesis of indole derivatives as novel α-glucosidase inhibitors in vitro. *Bioorg. Chem.* **2018**, *79*, 350–354. [CrossRef]
6. Sechi, M.; Derudas, M.; Dallocchio, R.; Dessi, A.; Bacchi, A.; Sannia, L.; Carta, F.; Palomba, M.; Ragab, O.; Chan, C.; et al. Design and synthesis of novel indole β-diketo acid derivatives as HIV-1 integrase inhibitors. *J. Med. Chem.* **2014**, *47*, 5298–5310. [CrossRef]
7. Al-Quawasmeh, R.A.; Huesca, M.; Nedunuri, V.; Peralta, R.; Wright, J.; Lee, Y.; Young, A. Potent antimicrobial activity of 3-(4,5-diaryl-1H-imidazol-2-yl)-1H-indole derivatives against methicillin-resistant Staphylococcus aureus. *Bioorg. Med. Chem. Lett.* **2010**, *20*, 3518–3520. [CrossRef]
8. Narayana, B.; Ashalatha, B.V.; Vijayaraj, K.K.; Fernandes, J.; Sarojini, B.K. Synthesis of some new biologically active 1, 3, 4-oxadiazolyl nitroindoles and a modified Fischer indole synthesis of ethyl nitro indole-2-carboxylates. *Bioorg. Med. Chem.* **2005**, *13*, 4638–4644. [CrossRef]
9. Ty, N.; Dupeyre, G.; Chabot, G.G.; Seguin, J.; Tillequin, F.; Scherman, D.; Michel, S.; Cachet, X. Synthesis and biological evaluation of new disubstituted analogues of 6-methoxy-3-(3′,4′,5′-trimethoxybenzoyl)-1H-indole (BPR0L075), as potential antivascular agents. *Bioorg. Med. Chem.* **2008**, *16*, 7494–7503. [CrossRef]
10. Bi, W.; Bi, Y.; Xue, P.; Zhang, Y.; Gao, X.; Wang, Z.; Li, M.; Baudy-Floc'h, M.; Ngerebara, N.; Gibson, K.M.; et al. Synthesis and characterization of novel indole derivatives reveal improved therapeutic agents for treatment of ischemia/reperfusion (I/R) injury. *J. Med. Chem.* **2010**, *53*, 6763–6767. [CrossRef]
11. Mascal, M.; Modes, K.V.; Durmus, A. Concise photochemical synthesis of the antimalarial indole alkaloid decursivine. *Angew. Chem. Int. Ed.* **2011**, *50*, 4445–4446. [CrossRef]
12. Huang, M.; Deng, Z.; Tian, J.; Liu, T. Synthesis and biological evaluation of salinomycin triazole analogues as anticancer agents. *Eur. J. Med. Chem.* **2017**, *127*, 900–908. [CrossRef] [PubMed]
13. Gujjar, R.; Marwaha, A.; El Mazouni, F.; White, J.; White, K.L.; Creason, S.; Shackleford, D.M.; Baldwin, J.; Charman, W.N.; Buckner, F.S.; et al. Identification of a metabolically stable triazolopyrimidine-based dihydroorotate dehydrogenase inhibitor with antimalarial activity in mice. *J. Med. Chem.* **2009**, *52*, 1864–1872. [CrossRef] [PubMed]
14. Chen, M.; Lu, S.; Yuan, G.; Yang, S.; Du, X. Synthesis and antibacterial activity of some heterocyclic β-enamino ester derivatives with 1,2,3-triazole. *Heterocycl. Commun.* **2000**, *6*, 421–426. [CrossRef]
15. Ayati, A.; Emami, S.; Foroumadi, A. The importance of triazole scaffold in the development of anticonvulsant agents. *Eur. J. Med. Chem.* **2016**, *109*, 380–392. [CrossRef]
16. Mohammad, Y.; Fazili, K.M.; Bhat, K.A.; Ara, T. Synthesis and biological evaluation of novel 3-O-tethered triazoles of diosgenin as potent antiproliferative agents. *Steroids* **2017**, *118*, 1–8.

17. Baburajeev, C.P.; Mohan, C.D.; Ananda, H.; Rangappa, S.; Fuchs, J.E.; Jagadish, S.; Siveen, K.S.; Chinnathambi, A.; Ali Alharbi, S.A.; Zayed, M.E.; et al. Development of novel triazolo-thiadiazoles from heterogeneous "green" catalysis as protein tyrosine phosphatase 1B inhibitors. *Sci. Rep.* **2015**, *5*, 14195. [CrossRef]
18. Timur, İ.; Kocyigit, Ü.M.; Dastan, T.; Sandal, S.; Ceribası, A.O.; Taslimi, P.; Gulcin, İ.; Koparir, M.; Karatepe, M.; Çiftçi, M. In vitro cytotoxic and in vivo antitumoral activities of some aminomethyl derivatives of 2,4-dihydro-3*H*-1,2,4-triazole-3-thiones—Evaluation of their acetylcholinesterase and carbonic anhydrase enzymes inhibition profiles. *J. Biochem. Mol. Toxic.* **2019**, *33*, e22239. [CrossRef]
19. Akhtar, T.; Hameed, S.; Khan, K.M.; Choudhary, M.I. Syntheses, urease inhibition, and antimicrobial studies of some chiral 3-substituted-4-amino-5-thioxo-1H,4H-1,2,4-triazoles. *Med. Chem.* **2008**, *4*, 539–543. [CrossRef]
20. Sevaille, L.; Gavara, L.; Bebrone, C.; De Luca, F.; Nauton, L.; Achard, M.; Mercuri, P.; Tanfoni, S.; Borgianni, L.; Guyon, C.; et al. 1,2,4-Triazole-3-thione compounds as inhibitors of dizinc metallo-β-lactamases. *ChemMedChem* **2017**, *12*, 972–985. [CrossRef]
21. Gavara, L.; Sevaille, L.; De Luca, F.; Mercuri, P.; Bebrone, C.; Feller, G.; Legru, A.; Cerboni, G.; Tanfoni, S.; Baud, D.; et al. 4-Amino-1, 2, 4-triazole-3-thione-derived Schiff bases as metallo-β-lactamase inhibitors. *Eur. J. Med. Chem.* **2020**, *208*, 112720. [CrossRef] [PubMed]
22. Boraei, A.T.A.; Soliman, S.M.; Yousuf, S.; Bibi, M.; Barakat, A. *N*-Acetyl Indole Linked to a Fused Triazolo/Thiadiazole Scaffold: Synthesis, Single Crystal X-Ray Structure, and Molecular Insight. *Crystals* **2020**, *10*, 600. [CrossRef]
23. Riyadh, S.M.; Abolibda, T.Z.; Sayed, A.R.; Gomha, S.M. Synthetic utility of aminomercapto [1,2,4] triazoles in the preparation of fused triazoles. *Curr. Org. Chem.* **2022**, *26*, 693–714.
24. Zhu, L.; Tang, S.Y.; Chen, D.P.; Li, C.P.; Shao, L.H.; Ouyang, G.P.; Wang, Z.C.; Li, Z.R. Synthesis and antibacterial activity of indole 3-substituted-[1,2,4] triazole derivatives. *Chem. Pap.* **2022**, *77*, 895–907. [CrossRef]
25. Dadlani, V.G.; Chhabhaiya, H.; Somani, R.R.; Tripathi, P.K. Synthesis, molecular docking, and biological evaluation of novel 1, 2, 4-triazole-isatin derivatives as potential Mycobacterium tuberculosis shikimate kinase inhibitors. *Chem. Biol. Drug Des.* **2022**, *100*, 230–244. [CrossRef] [PubMed]
26. Trafalis, D.T.; Sagredou, S.; Dalezis, P.; Voura, M.; Fountoulaki, S.; Nikoleousakos, N.; Almpanakis, K.; Deligiorgi, M.V.; Sarli, V. Anticancer Activity of Triazolo-Thiadiazole Derivatives and Inhibition of AKT1 and AKT2 Activation. *Pharmaceutics* **2021**, *13*, 493. [CrossRef] [PubMed]
27. Liu, X.J.; Liu, H.Y.; Wang, H.X.; Shi, Y.P.; Tang, R.; Zhang, S.; Chen, B.Q. Synthesis and antitumor evaluation of novel fused heterocyclic 1, 2, 4-triazolo [3, 4-b]-1, 3, 4-thiadiazole derivatives. *Med. Chem. Res.* **2019**, *28*, 1718–1725. [CrossRef]
28. Boraei, A.T.; Singh, P.K.; Sechi, M.; Satta, S. Discovery of novel functionalized 1, 2, 4-triazoles as PARP-1 inhibitors in breast cancer: Design, synthesis and antitumor activity evaluation. *Eur. J. Med. Chem.* **2019**, *182*, 111621. [CrossRef]
29. Boraei, A.T.A.; Sarhan, A.A.M.; Yousuf, S.; Barakat, A. Synthesis of a New Series of Nitrogen/Sulfur Heterocycles by Linking Four Rings: Indole; 1,2,4-Triazole; Pyridazine; and Quinoxaline. *Molecules* **2020**, *25*, 450. [CrossRef]
30. Sarhan, A.A.; Boraei, A.T.; Barakat, A.; Nafie, M.S. Discovery of hydrazide-based pyridazino [4,5-b] indole scaffold as a new phosphoinositide 3-kinase (PI3K) inhibitor for breast cancer therapy. *RSC Adv.* **2020**, *10*, 19534–19541. [CrossRef]
31. Rikagu Oxford Diffraction. *CrysAlisPro*; Rikagu Oxford Diffraction Inc.: Yarnton, UK, 2020.
32. Sheldrick, G.M. SHELXT-Integrated Space-Group and Crystal-Structure Determination. *Acta Crystallogr. Sect. A Found. Adv.* **2015**, *71*, 3–8. [CrossRef] [PubMed]
33. Sheldrick, G.M. Crystal structure refinement with SHELXL. *Acta Cryst. C* **2015**, *71*, 3–8. [CrossRef] [PubMed]
34. Hübschle, C.B.; Sheldrick, G.M.; Dittrich, B.J. ShelXle: A Qt graphical user interface for SHELXL. *J. Appl. Cryst.* **2011**, *44*, 1281–1284. [CrossRef]
35. Turner, M.J.; McKinnon, J.J.; Wolff, S.K.; Grimwood, D.J.; Spackman, P.R.; Jayatilaka, D.; Spackman, M.A. Crystal Explorer17 University of Western Australia. 2017. Available online: http://hirshfeldsurface.net (accessed on 31 July 2021).
36. Dey, D.; Bhandary, S.; Thomas, S.P.; Spackman, M.A.; Chopra, D. Energy frameworks and a topological analysis of the supramolecular features in in situ cryocrystallized liquids: Tuning the weak interaction landscape via fluorination. *Phys. Chem. Chem. Phys.* **2016**, *18*, 31811–31820. [CrossRef] [PubMed]
37. Miroslaw, B.; Demchuk, O.M.; Luboradzki, R.; Tyszczuk-Rotko, K. Low-Molecular-Weight Organogelators Based on N-dodecanoyl-L-amino Acids—Energy Frameworks and Supramolecular Synthons. *Materials* **2023**, *16*, 702. [CrossRef] [PubMed]